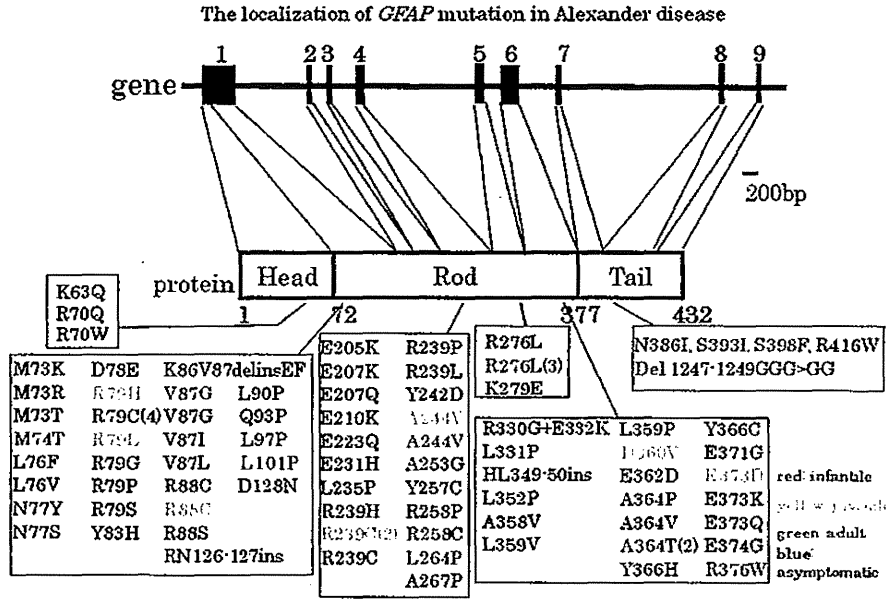

Fig. 2 Schematic demonstrating the *GFAP*, corresponding proteins, and localization of *GFAP* mutations in AxD. Colors indicate mutations reported in this survey: *red* infantile AxD, *yellow* juvenile AxD, *green* adult AxD, *blue* asymptomatic individuals. Mutations shown in *black* indicate published *GFAP* mutations that were excluded from this survey

Although white matter abnormalities were observed in all juvenile AxD patients, abnormalities of the basal ganglia and thalami, periventricular rim, and abnormalities of the brainstem were only observed in approximately 50% of these patients.

Gene analysis is summarized in Fig. 2. *Glial fibrillary acidic protein* analysis was performed for all 35 AxD patients. The mutation sites were unknown for five cases despite the existence of genetic abnormalities, because each patient underwent gene analysis at different facilities; hence a total of 30 patients were available for further analysis. All mutations were identified as *GFAP* point mutations except for one infantile AxD patient, who showed one base deletion in exon 7. The residues affected by point mutation in 70.0% of infantile AxD patients included R79, R88, and R239. Amino acid mutations in juvenile AxD included mutations at R79, R88, R239, A244, D360, and E373. Mutations detected in adult AxD were spread throughout *GFAP* and included M74T, V87G, L101P, A244V, L264P, R258C, R276L, A364T, R376W, S393I, and S398F. The A244V mutation was detected in juvenile and adult AxD.

Electrophysiological findings, treatments, and prognosis are summarized in Table 5. Electroencephalogram (EEG) recordings revealed abnormalities in 8 of 9 (88.9%) infantile AxD patients, 6 of 7 (85.7%) juvenile AxD patients, and 6 of 13 (46.2%) adult AxD patients. Auditory brainstem response (ABR) findings revealed abnormalities in four of five (80.0%) infantile AxD patients, five of seven (71.4%) juvenile AxD patients, and four of five (80.0%) adult AxD patients. Nerve conduction studies were conducted in 13 adult AxD patients, which revealed abnormalities in motor and sensory nerve conduction in 4 (30.8%) and 2 (15.4%) of these patients, respectively. However, data for these studies contained information only about whether it was normal or abnormal. There was no information about the sites of examination or details of the abnormalities.

The survey results did not specify any therapy for AxD. However, some symptomatic treatments were described and evaluated. Antiepileptic drugs seemed to be effective for treating convulsions in infantile or juvenile AxD patients. The efficacy of thyroid-releasing hormone (TRH) therapy was evaluated in three patients, being effective for treating ataxia and some brainstem abnormalities in one juvenile AxD patient. In this patient, envelope-area improvement was observed by balance testing using a stabilometer. Two adult AxD patients were treated with L-dopa, an antiparkinsonism drug, and one adult AxD patient was treated with tizanidine, an antispasticity drug.

The disease duration of the surviving cases ranged from 7 months to 18 years for infantile AxD, from 4 years 6 months to 21 years for juvenile AxD, and from 1 to 16 years for adult AxD patients. Nine of the ten infantile AxD patients were still alive and receiving home care when the first survey was conducted. All juvenile AxD patients were also alive; seven were receiving home care, and one was undergoing treatment in a hospital. Three adult AxD patients failed to survive, and 13 were alive. There was no information on one patient. One nonsurvival case was a patient with V87G who died at the age of 67 years with disease duration of 13 years. In the second case, a patient with R276L died at the age of 51 years with disease duration of 18 years. In the third case, the patient with R258C died at the age of 77 years with disease duration of 9 years.

Table 5 Summary of abnormalities of electrophysiological examinations, therapy, and prognosis in the second survey

	Infantile form	Juvenile form	Adult form
Abnormalities of electrophysiological examinations			
Motor nerve conduction study	0% (0/5)	0% (0/4)	30.8% (4/13)
Sensory nerve conduction study	0% (0/3)	0% (0/2)	15.4% (2/13)
Electroencephalogram	88.9% (8/9)	85.7% (6/7)	46.2% (6/13)
Sensory evoked potential	100% (2/2)	50.0% (2/4)	42.9% (3/7)
Motor evoked potential	100% (1/1)		100% (3/3)
Auditory brainstem response	80.0% (4/5	71.4% (6/7)	80.0% (4/5)
Visual evoked potential	100% (2/2)	50.0% (12)	50.0% (12)
Therapy			
Antiepileptic drugs	8 cases (7 were effective)	3 cases (all were effective)	2 cases (1 was effective)
TRH	1 case	1 case (effective)	1 case
Other			L-Dopa antispasticity dugs
Prognosis	9 cases: alive	8 cases: alive	13 cases: alive
	1 case unknown		3 cases: dead
			1 case: unknown

Discussion

A definitive diagnosis of Alexander disease requires genetic analysis or pathological diagnosis, and diagnoses are almost exclusively given by neurologists or neuropediatricians. Therefore, the estimated number of patients was reported as (patients in the second survey)/(sampling rate × response rate in the first survey) = (reported number of patients)/(response rate in first survey) = 35/0.74 = 47 patients, which is a minimal prevalence assuming that it is unlikely that other units have diagnosed AxD. Considering that the population in Japan is approximately 128 million, we estimate that the disease prevalence is approximately 1 in 2.7 million people, which indicates the frequency of AxD for a 5-year period. The number of actual patients indicates only the number reported in this study, and does not include affected family members who were not reported. Also, the time parameter for prevalence was 5 years, which was also the duration of investigation for this study. Although genetic testing for AxD is mainly conducted in the facility where the present authors work, we cannot rule out the existence of uncertain cases because of the small number of Japanese facilities that conduct genetic testing for AxD. Therefore, the actual prevalence may possibly be higher than that indicated by this study.

Regarding the frequency of the various forms of the disease, adult AxD accounted for 48.5% of the total cases evaluated in this study, and was the most frequent form reported in the survey. However, it was previously reported that infantile AxD accounts for 51% of the total number of AxD cases and is the most frequent form, while adult AxD is the least frequent form, accounting for only 27.2% of total cases [12]. Nevertheless, we consider the results of the present study to be reliable, based on the high response rate to both the first and the second survey. Adult AxD is more difficult to diagnose than infantile AxD, because the MRI criteria and typical clinical symptoms in infantile AxD patients show more regions of brain involvement [11]. Therefore, the frequency of occurrence of adult AxD is not related to that of diagnosis of infantile AxD patients.

We based this study on the presently conducted surveys. However, one case of infantile AxD (1247-1249GGG>GG [13]), two cases of juvenile AxD (D360V [14], R79H [15]), and nine cases of adult AxD (S398F [16], L264P [17], V87G [18], R276L [19, 20], R376W [21], L101P [22], R258C [23], and M74T [24]) have been previously reported. Two cases included in this study, A364T (juvenile AxD) and E373D (adult AxD), are new variations that have not been previously reported.

Cerebral symptoms, such as delayed psychomotor development or mental retardation, convulsions, and macrocephaly, are the most significant neurological findings considered for the diagnosis of infantile AxD. The general characteristics of AxD on brain MRI include predominant cerebral white matter abnormalities in the frontal lobe, signal abnormalities indicating swelling or atrophy of the basal ganglia and thalami, and periventricular rim. Furthermore, progressive bulbospinal symptoms, such as bulbar signs, motor signs, and autonomic dysfunction, may aid

diagnosis of adult AxD. Characteristic findings on MRI in adult AxD patients included signal abnormalities and/or atrophy of medulla oblongata and cervical spinal cord, and abnormalities of other structures related to the brainstem and cerebellum. These results support the results of previous MRI studies [7–9, 23].

Glial fibrillary acidic protein mutations at R79, R88, and R239 accounted for 75.0% of mutations identified in infantile and juvenile AxD patients; however, these mutations were not detected in any of the adult AxD cases. The abnormalities at R79, R88, and R239, which are reported worldwide, have a tendency to be associated with infantile or juvenile AxD. R79 mutations are reported in adult AxD patients, although this is rare [23]. Approximately 60% of the *GFAP* mutations identified in adult AxD cases in this survey were only detected in the Japanese population. Sixty-five percent of adult AxD patients had family members with AxD. In contrast, infantile or juvenile AxD patients had no family histories of AxD, except for one pair of twins. The R276L mutation was observed in three independent families from the same region of Japan. This mutation was not a mutational site with many known cases seen across different races, such as R79 and R239, but was observed in cases found in the same area. Although we cannot rule out that it was a de novo mutation, this mutation is suggestive of the founder effect. Two unrelated patients from the same prefecture in the northern part of Japan were identified with the A244V mutation. However, this mutation was also observed in a patient of other race [6]. Therefore, the A244V mutation may not be the result of a founder effect in Japan.

All infantile or juvenile AxD patients suffered seizures and hence showed EEG abnormalities. However, approximately 50% of adult AxD patients also showed EEG abnormalities, suggesting subclinical cerebral dysfunction resulting from pathological abnormalities in the cerebral matter. ABR abnormalities were independent of AxD type, indicating that radiological and pathological abnormalities of medulla oblongata were observed in all AxD types.

Unfortunately, this survey did not specify any therapies for AxD. However, antiepileptic drugs were reported to be effective in controlling seizures, although seizures that present in infantile or juvenile AxD are considered intractable. The efficacy of TRH therapy was evaluated in three patients. Thyroid-releasing hormone is a neuromodulator of the cerebellum and brainstem and is expected to improve cerebellar ataxia and symptoms of brainstem dysfunction [14]. However, the effectiveness of TRH needs to be confirmed by further large-scale studies. Ceftriaxone, which was not reported in this survey, was recently reported as a potential therapy for halting the progression of some neurological symptoms of AxD [25, 26].

The prognosis of AxD was reported to be relatively good in this survey, which may be due to various reasons. First neonatal AxD, which results in severe disability or death within 2 years [12], was not reported. Second, improvements in general care, nutritional requirements, and respiratory care have contributed to extending the lifespan of AxD patients. However, most patients with AxD receive care in their own homes; therefore, better care is required for such patients.

We inferred the prevalence of AxD in Japan from the high response rate achieved in both our studies. However, we cannot rule out that there may be more than a few undiagnosed cases, one reason being the lack of enough facilities that perform genetic testing for definitive diagnosis of the disease. Another reason is that diagnosis of juvenile AxD may be difficult, particularly in Japan. This is supported by the fact that, in our first survey, no cases of onset during the teens (there are no reports of this originating in Japan) were found, which may be due to several reasons. First, extremely varied cases were found such as cases that presented clinical features of infantile AxD, of adult AxD, of both, and even cases that presented changes in medulla oblongata and cervical spinal cord but that were seen as tuberous in imaging findings [27–29]. These variations may lead to confusion among physicians and misdiagnosis. Second, in Japan, patients in their teens are examined by pediatricians, and MRI diagnostic standards established by van der Knaap et al. [11] are very well known, hence symptoms that are similar to adult AxD, which falls outside those guidelines, may be overlooked. We also inferred this because no such cases of juvenile AxD were reported. Furthermore, although neurologists usually diagnose cases in older teens, we speculate that some cases of AxD are confused for other diseases (such as multiple sclerosis or cancer). This confusion could be similar to cases of nodular lesions that do not present with atrophy, but rather are believed to be observed in juvenile AxD, when patients present atrophy of medulla oblongata or cervical spinal cord, or in cases where signal abnormality that accompanies atrophy indicates possible adult AxD [8, 9, 23]. Therefore, to ensure correct diagnosis of AxD, the physician should understand the importance of the process of *GFAP* genetic testing, which provides definitive diagnosis, but before that the neuropediatrician and neurologist should understand the importance of suspecting AxD from the patient's clinical condition and MRI findings, and place high importance on identifying juvenile AxD, which presents the most complex clinical features. For this reason, we believe that a new classification that helps physicians to suspect AxD based only on neurological and neuroradiological findings, instead of the age at which symptoms present, would be beneficial.

Table 6 Guideline for diagnosing Alexander disease

1. Cerebral Alexander disease (type 1)
I. Neurological findings
(a) Core features
Psychomotor developmental delay/mental retardation, convulsions, macrocephaly
(b) Supportive features
Dysarthria, dysphagia, dysphonia, hyperreflexia, cerebellar ataxia, sphincter abnormalities, scoliosis
II. MRI findings
(a) Core feature
Cerebral white matter abnormalities with frontal lobe predominance
(b) Supportive features
Signal abnormalities with swelling or atrophy of basal ganglia and thalami, periventricular rim, brainstem lesions, contrast enhancement
2. Bulbospinal Alexander disease (type 2)
I. Neurological findings
(a) Core features
Muscle weakness, hyperreflexia (sometimes hypo- or areflexia), positive Babinski sign, dysarthria, dysphagia, dysphonia
(b) Not frequent but specific features
Palatal myoclonus
(c) Supportive features
Cerebellar ataxia nystagmus, scoliosis, sleep disorder (i.e., sleep apnea syndrome, REM behavior disorder), parkinsonism, dementia, psychosis, sphincter abnormalities
II. MRI findings
(a) Core feature
Signal abnormalities or atrophy of medulla oblongata and/or cervical cord
(b) Supportive features
Signal abnormalities and/or atrophy of cerebellum, white matter lesion, signal abnormalities of basal ganglia and thalami, contrast enhancement
3. Intermediate form (type 3)
I. Neurological findings
At least one of the core features in type 1 and at least one of the core features in type 2
II. MRI findings
Core feature of type 1 and core feature of type 2
For a case satisfying any of the above-mentioned types, the following definite diagnosis is recommended
Definite diagnosis
I. Pathological findings
Existence of numerous Rosenthal fibers in addition to gliosis and loss of myelin
II. Gene analysis
GFAP mutation

Approximately 10% of Alexander disease cases seem to show negative *GFAP* mutation in spite of showing typical clinical features of Alexander disease and pathological findings. Therefore, cases satisfying the above clinical features but with negative *GFAP* mutation may be Alexander disease ("possible" Alexander disease)

Based on the above findings, we propose a new guideline where the clinical forms of AxD are classified into the following three types based on neurological and MRI findings: (1) cerebral (type 1), (2) bulbospinal AxD (type 2), and (3) intermediate form (type 3) (Table 6). The primary objective of our guidelines is to increase diagnostic yield by suspecting AxD based on neurological symptoms and MRI findings, which will lead to genetic or pathological testing. Hence, we decided to increase the sensitivity instead of increasing the positive predictive value. On the basis of these new guidelines, we have corrected and updated the neurological and MRI findings for the cases included in our study (Table 7, 8) to 12 cases of type 1 (previously, 9 cases were classified as infantile AxD and 3 as juvenile AxD), 16 cases of type 2 (all cases were previously classified as adult AxD), and 7 cases of type 3 (previously, 1 case was classified as infantile AxD, 5 cases as juvenile AxD, and 1 case as adult AxD).

The phenotypes may seem to vary greatly between type 1 and type 2, but from changes in the images of

Table 7 Summary of neurological signs of Alexander disease classified by the proposed guideline

	Type 1 ($n = 12$)	Type 2 ($n = 16$)	Type 3 ($n = 7$)
Age at onset	3 m to 5 y	26 to 61 y	9 m to 30 y
Muscle weakness	33.0% (1/3)	87.5% (14/16)	60.0% (3/5)
Tendon reflex abnormality	77.8% (7/9)	93.8% (15/16)	83.3% (5/6)
Hyperreflexia	77.8% (6/9)	93.8% (15/1)	83.3% (5/6)
Hyporeflexia or areflexia		12.5% (2/16)	
Babinski sign	33.0% (1/3)	81.3% (13/16)	80.0% (4/5)
Parkinsonism	0.0% (0/3)	25.0% (4 16)	20.0% (1/5)
Sensory disturbance	0.0% (0/3)	18.8% (3/16)	0.0% (0/5)
Dysarthria	100.0% (8/8)	87.5% (14/16)	100.0% (7/7)
Dysphonia	63.8% (7/11)	68.8% (11/16)	42.9% (3/7)
Dysphagia	54.5% (6/11)	87.5% (14/16)	57.1% (4/7)
Nystagmus	0.0% (0/8)	68.8% (11/16)	0.0% (0/7)
Limb ataxia	14.3% (1/7)	33.3% (4/12)	42.9% (3/7)
Truncal ataxia	0.0% (0/7)	50.0% (6/12)	83.3% (5/6)
Palatal myoclonus	0.0% (0/8)	40.0% (6/15)	0.0% (0/6)
Orthostatic hypotension	0.0% (0/3)	7.7% (1/13)	50.0% (1/2)
Sphincter abnormalities	27.3% (3/11)	53.8% (7/13)	28.6% (2/7)
Sleep disorder	0.0% (0/2)	30.8% (4/13)	50.0% (1/2)
Convulsions	90.9% (10/11)	0.0% (0/15)	100.0% (7/7)
Mental retardation/psychomotor developmental delay	90.0% (9/10)	0.0% (0/15)	100.0% (7/7)
Dementia		26.7% (4/15)	0.0% (0/1)
Macrocephaly	80.0% (8/10)		50.0% (3/6)
Scoliosis	45.5% (5/11)	13.3% (2/15)	50.0% (3/6)

Table 8 Summary of MRI findings of Alexander disease classified by the proposed guideline

	Type 1 ($n = 12$)	Type 2 ($n = 16$)	Type 3 ($n = 7$)
White matter lesion	100.0% (12/12)	33.3% (5/15)	100.0% (7/7)
Abnormalities of basal ganglia, thalamus	81.8% (9/11)	46.7% (7/15)	71.4% (5/7)
Abnormalities of brainstem			
Medulla oblongata	0.0% (0/9)	100.0% (15/15)	100.0% (7/7)
Pons	0.0% (0/9)	73.3% (11/15)	100.0% (7/7)
Midbrain	11.1% (1/9)	73.3% (11/15)	100.0% (6/6)
Abnormalities of cervical cord	0.0% (0/6)	100.0% (15/15)	75.0% (3/4)
Abnormalities of cerebellum	20.0% (2/10)	60.0% (9/15)	94.3% (6/7)
Periventricular rim	77.8% (7/9)	26.7% (4/15)	94.3% (6/7)
Enhancement	66.7% (4/6)	8.3% (1/12)	

recently reported long-term survival infantile cases [30], and from the progression of medulla oblongata and cervical spinal cord atrophy seen in an adult cases [31], we believe that certain factors related to the developmental stage determine the severity of cerebral white matter pathological change.

In conclusion, we report a large number of AxD patients in Japan, and provide an estimate of the overall prevalence of the disease with relative frequencies of the three forms. In addition, we propose new clinical guidelines for diagnosing AxD based on simplified classifications. We hope that this report and the guidelines we propose will lead to higher diagnostic yield in the future.

Acknowledgments This work was supported by Alexander disease research grants received from the Intractable Disease Research Grants, from the Ministry of Health, Labor, and Welfare of the Government of Japan, and a Grant-in-Aid for Young Scientists (B) from the Ministry of Education, Culture, Sports, Science, and Technology of Japan (grant number 22790825).

Conflicts of interest None.

Appendix

The Alexander Disease Study Group in Japan: Manami Akasaka, MD (Iwate Medical University); Nobutaka Sakae, MD (Kyusyu University); Hitoshi Yamamoto, MD (St. Marianna University of Medicine); Toshiro Okazaki, MD (Oita University); Yasuhiro Takeshima, MD (Kobe University); Keiji Senda, MD (National Hospital Organization Iwate Hospital); Nobuyuki Murakami, MD (Dokkyo Medical University Koshigaya Hospital); Takayoshi Shimohata, MD (Niigata University); Ryutarou Kohira, MD (Nihon University Itabashi Hospital); Tomoaki Yuhi, MD (University of Occupational and Environmental Health); Akira Sudo, MD (Sapporo City General Hospital); Ikuko Aiba, MD (National Hospital Organization Higashi Nagoya Hospital); Keiko Ishigaki, MD (Tokyo Woman's Medical University, School of Medicine); Hisato Nakamura, MD (Iwao Hospital); Hiroko Tsukamoto, MD (Sumitomo Hospital); Hideki Houzen, MD (Obihiro General Hospital); Koki Nikaido, MD (Sapporo Medical University); Yoshihiro Suzuki, MD (Nihonkai General Hospital); Hitoshi Kawato, MD (Asahi Hospital); Yasushi Kita, MD (Hyogo Brain and Heart Center); Hitoshi Osaka, MD (Kanagawa Children's Medical Center); Toru Yamamoto, MD (Osaka Saiseikai Nakatsu Hospital); Atsushi Imamura, MD (Gifu Prefectural General Medical Center); Hideaki Kishikawa, MD (Kahan Hospital); Muneaki Matsuo, MD (Saga University); Rei Masuda, MD (Kitasato University School of Medicine); Mitsugu Uematsu, MD (Tohoku University); Hasegawa Kazuko, MD (National Hospital Organization Sagamihara); Tadataka Hoshika, MD (Tottori Prefectural General Medical Center); Hiroaki Shii, MD (Kokura Memorial Hospital); Takashi Shiihar, MD (Gunma Children's Medical Center); Michio Kobayashi, MD (National Hospital Organization Akita Hospital); Kazuhiro Takamatsu, MD (Oota Memorial Hospital); Takahiro Yokoyama, MD (Yotsuya Medical Mall); Yasuyuki Okuma, MD (Juntendo University Shizuoka Hospital); Kazuhide Ochi, MD (Hiroshima University); Kazuma Kaneko, MD (Shinsyu University).

References

1. Alexander WS (1949) Progressive fibrinoid degeneration of fibrillary astrocytes associated with mental retardation in a hydrocephalic infant. Brain 72:373–381
2. Iwaki T, Kume-Iwaki A, Liem RKH, Goldman JE (1989) Alpha-B-crystallin is expressed in non-lenticular tissues and accumulates in Alexander's disease brain. Cell 57:71–78
3. Iwaki T, Iwaki A, Tateishi J, Sasaki Y, Goldman JE (1993) Alpha B-crystallin and 27-kDa heat shock protein are regulated by stress conditions in the nervous system and accumulate in Rosenthal fibers. Am J Pathol 143:487–495
4. Brenner M, Johnson AB, Boespflug-Tanguy O, Rodriguez D, Goldman JE, Messing A (2001) Mutations in *GFAP*, encoding glial fibrillary acidic protein, are associated with Alexander disease. Nat Genet 27:277–286
5. Rodriguez D, Gauthier F, Bertini E, Bugiani M, Brenner M, N'guyen S, Goizet C, Gelot A, Surtees R, Pedespan JM, Hernandorena X, Troncoso M, Uziel G, Messing A, Ponsot G, Pham-Dinh D, Dautigny A, Boespflug-Tanguy O (2001) Infantile Alexander disease: spectrum of GFAP mutations and genotype-phenotype correlation. Am J Hum Genet 69:1134–1140
6. Li R, Johnson AB, Salomons G, Rodriguez D, Goldman JE, Messing A (2005) Glial fibrillary acidic protein mutations in infantile, juvenile, and adult forms of Alexander disease. Ann Neurol 57:310–326
7. van der Knaap MS, Ramesh V, Schiffmann R, Blaser S, Kyllerman M, Gholkar A, Ellison DW, van der Voorn JP, van Dooren SJM, Jakobs C, Barkhof F, Salomons GS (2006) Alexander disease. Ventricular garlands and abnormalities of the medulla and spinal cord. Neurology 66:494–498
8. Farina L, Pareyson D, Minati L, Ceccherini I, Chiapparini L, Romano S, Gambaro P, Fancellu R, Savoiardo M (2008) Can MR imaging diagnose adult-onset Alexander disease? Am J Neuroradiol 29:1190–1196
9. Pareyson D, Fancellu R, Mariotti C, Romano S, Salmaggi A, Carella F, Girotti F, Gattellaro G, Carriero MR, Farina L, Ceccherini I, Savoiardo M (2008) Adult-onset Alexander disease: a series of eleven unrelated cases with review of the literature. Brain 131:2321–2331
10. Balbi P, Salvini S, Fundarò C, Frazzitta G, Maestri R, Mosah D, Uggetti C, Sechi G (2010) The clinical spectrum of late-onset Alexander disease: a systematic literature review. J Neurol 257:1955–1962
11. van der Knaap MS, Naidu S, Breiter SN, Blaser S, Stroink H, Springer S, Begger JC, van Coster R, Barth PG, Thomas NH, Valk J, Powers JM (2001) Alexander disease: diagnosis with MR imaging. Am J Neuroradiol 22:541–552
12. Gorospe JR (2010) Alexander disease. GeneReviews(Internet). Updated 2010 Apr 22
13. Murakami N, Tsuchiya T, Kanazawa N, Tsujino S, Nagai T (2008) Novel deletion mutation in GFAP gene in an infantile form of Alexander disease. Pedatr Neurol 38:50–52
14. Ishigaki K, Ito Y, Sawaishi Y, Kodaira K, Funatsuka M, Hattori N, Nakano K, Saito K, Osawa M (2006) TRH therapy in a patient with juvenile Alexander disease. Brain Dev 28:663–667
15. Asahina N, Okamoto T, Sudo A, Kanazawa N, Tsujino S, Saitoh S (2006) An infantile-juvenile form of Alexander disease caused by a R79H mutation in *GFAP*. Brain Dev 28:131–133
16. Sueda Y, Takahashi T, Ochi K, Ohtsuki T, Namekawa M, Kohriyama T, Takiyama Y, Matsumoto M (2009) Adult onset Alexander disease with a novel variant (S398F) in the glial fibrillary acidic protein gene. Clin Neurol 49:358–363
17. Ayaki T, Shinohara M, Tatsumi S, Namekawa M, Yamamoto T (2010) A case of sporadic adult Alexander disease presenting with acute onset, remission and relapse. J Neurol Neurosurg Psychiatry 81:1292–1293
18. Okamoto Y, Mitsuyama H, Jonosono M, Hirata K, Arimura K, Osame M, Nakagawa M (2002) Autosomal dominant palatal myoclonus and spinal cord atrophy. J Neurol Sci 19:71–76
19. Namekawa M, Takiyama Y, Aoki Y, Takayashiki N, Sakoe K, Shimazaki H, Taguchi T, Tanaka Y, Nishizawa M, Saito K, Matsubara Y, Nakano I (2002) Identification of GFAP gene mutation in hereditary adult-onset Alexander's disease. Ann Neurol 52:779–785
20. Namekawa M, Takiyama Y, Honda J, Shimazaki H, Sakoe K, Nakano I (2010) Adult-onset Alexander disease with typical "tadpole" brainstem atrophy and unusual bilateral basal ganglia

involvement: a case report and review of the literature. BMC Neurol 10:21
21. Hirayama T, Fukue J, Noda K, Fujishima K, Yamamoto T, Mori K, Maeda M, Hattori N, Shiroma N, Tsurui S, Okuma Y (2008) Adult-onset Alexander disease with palatal myoclonus and intraventricular tumor. Eur J Neurol 15:16–17
22. Kaneko H, Hirose M, Katada S, Takahashi T, Naruse S, Tsuchiya M, Yoshida T, Onodera O, Nishizawa M (2009) Novel GFAP mutation in patient with adult-onset Alexander disease presenting with spastic ataxia. Mov Dis 24:1393–1395
23. Yoshida T, Sasayama H, Mizuta I, Okamoto Y, Yoshida M, Riku Y, Hayashi Y, Yonezu T, Takata Y, Ohnari K, Nakagawa M (2010) Glial fibrillary acidic protein mutations in adult-onset Alexander disease: clinical features observed in 12 Japanese cases. Acta Neurol Scand published online
24. Ohnari K, Yamano M, Uozumi T, Hashimoto T, Tsuji S, Nakagawa M (2007) An adult form of Alexander disease: novel mutation in glial fibrillary acidic protein. J Neurol 254:1390–1394
25. Sechi G, Matta M, Deiana GA, Balbi P, Bachetti T, Di Zanni E, Ceccherini I, Serra A (2010) Ceftriaxone has a therapeutic role in Alexander disease. Pro Neuropsy Biol Psychi 34:416–417
26. Bachetti T, Di Zanni E, Balbi P, Bocca P, Prigione I, Deiana GA, Rezzani A, Ceccherini I, Sechi G (2010) In vitro treatments with ceftriaxone promote elimination of mutant glial fibrillary acidic protein and transcription down-regulation. Exp Cell Res 316:2152–2165
27. Probst EN, Hagel C, Weisz V, Nagel S, Wittkugel O, Zeumer H, Kohlschötter A (2003) Atypical focal MRI lesions in a case of juvenile Alexander's disease. Ann Neurol 53:118–120
28. van der Knaap MS, Salomons GS, Li R, Franzoni E, Gutiérrez-Solana LG, Smit LME, Robinson R, Ferrie CD, Cree B, Reddy A, Thomas N, Banwell B, Barkhof F, Jakobs C, Johnson A, Messing A, Brenner M (2005) Unusual variants of Alexander's disease. Ann Neurol 57:327–338
29. Niinikoski H, Haataja L, Brander A, Valanne L, Blaser S (2009) Alexander disease as a cause of nocturnal vomiting in a 7-year-old girl. Pediatr Radiol 39:872–875
30. Shiihara T, Yoneda T, Mizuta I, Yoshida T, Nakagawa M, Shimizu N (2010) Serial MRI changes in a patient Alexander disease and prolonged survival. published online Oct 30 2010
31. Romano S, Salvetti M, Ceccherini I, De Simone T, Savoiardo M (2007) Brainstem signs with progressing atrophy of medulla oblongata and upper cervical cord. Lancet Neurol 6:562–570

REPORT

The TRK-Fused Gene Is Mutated in Hereditary Motor and Sensory Neuropathy with Proximal Dominant Involvement

Hiroyuki Ishiura,[1] Wataru Sako,[3] Mari Yoshida,[4] Toshitaka Kawarai,[3] Osamu Tanabe,[3,5] Jun Goto,[1] Yuji Takahashi,[1] Hidetoshi Date,[1] Jun Mitsui,[1] Budrul Ahsan,[1] Yaeko Ichikawa,[1] Atsushi Iwata,[1] Hiide Yoshino,[6] Yuishin Izumi,[3] Koji Fujita,[3] Kouji Maeda,[3] Satoshi Goto,[3] Hidetaka Koizumi,[3] Ryoma Morigaki,[3] Masako Ikemura,[7] Naoko Yamauchi,[7] Shigeo Murayama,[8] Garth A. Nicholson,[9] Hidefumi Ito,[10] Gen Sobue,[11] Masanori Nakagawa,[12] Ryuji Kaji,[3,*] and Shoji Tsuji[1,2,13,*]

Hereditary motor and sensory neuropathy with proximal dominant involvement (HMSN-P) is an autosomal-dominant neurodegenerative disorder characterized by widespread fasciculations, proximal-predominant muscle weakness, and atrophy followed by distal sensory involvement. To date, large families affected by HMSN-P have been reported from two different regions in Japan. Linkage and haplotype analyses of two previously reported families and two new families with the use of high-density SNP arrays further defined the minimum candidate region of 3.3 Mb in chromosomal region 3q12. Exome sequencing showed an identical c.854C>T (p.Pro285-Leu) mutation in the TRK-fused gene (*TFG*) in the four families. Detailed haplotype analysis suggested two independent origins of the mutation. Pathological studies of an autopsied patient revealed TFG- and ubiquitin-immunopositive cytoplasmic inclusions in the spinal and cortical motor neurons. Fragmentation of the Golgi apparatus, a frequent finding in amyotrophic lateral sclerosis, was also observed in the motor neurons with inclusion bodies. Moreover, TAR DNA-binding protein 43 kDa (TDP-43)-positive cytoplasmic inclusions were also demonstrated. In cultured cells expressing mutant TFG, cytoplasmic aggregation of TDP-43 was demonstrated. These findings indicate that formation of TFG-containing cytoplasmic inclusions and concomitant mislocalization of TDP-43 underlie motor neuron degeneration in HMSN-P. Pathological overlap of proteinopathies involving TFG and TDP-43 highlights a new pathway leading to motor neuron degeneration.

Hereditary motor and sensory neuropathy with proximal dominant involvement (HMSN-P [MIM 604484]) is an autosomal-dominant disease characterized by predominantly proximal muscle weakness and atrophy followed by distal sensory disturbances.[1] HMSN-P was first described in patients from the Okinawa Islands of Japan, where more than 100 people are estimated to be affected.[2] Two Brazilian HMSN-P-affected families of Okinawan ancestry have also been reported.[3,4]

The disease onset is usually in the 40s and is followed by a slowly progressive course. Painful muscle cramps and abundant fasciculations are observed, particularly in the early stage of the disease. In contrast to the clinical presentations of other hereditary motor and sensory neuropathies (HMSNs) presenting with predominantly distal motor weakness reflecting axonal-length dependence, the clinical presentation of HMSN-P is unique in that it involves proximal predominant weakness with widespread fasciculations resembling those of amyotrophic lateral sclerosis (ALS).[5] Distal sensory loss is accompanied later in the disease course, but the degree of the sensory involvement varies among patients. Neuropathological findings revealed severe neuronal loss and gliosis in the spinal anterior horns and mild neuronal loss and gliosis in the hypoglossal and facial nuclei of the brainstem, which indicates that the primary pathological feature of HMSN-P is a motor neuronopathy involving motor neurons, but not a motor neuropathy involving axons.[1,5] The posterior column, corticospinal tract, and spinocerebellar tract showed loss of myelinated fibers and gliosis. Neuronal loss and gliosis were found in Clarke's nucleus. Dorsal root ganglia showed mild to marked neuronal loss.[1,5] These observations suggest that HMSN-P shares neuropathological findings in part with those observed in familial ALS.[6]

Previous studies on Okinawan kindreds mapped the disease locus to chromosome 3q.[1] Subsequently, we identified two large families (families 1 and 2 in Figure 1A) affected by quite a similar phenotype in the Kansai area of Japan, located in the middle of the main island of Japan and far distant from the Okinawa Islands. We mapped the

[1]Department of Neurology, The University of Tokyo Graduate School of Medicine, 7-3-1 Hongo, Bunkyo-ku, Tokyo 113-8655, Japan; [2]Medical Genome Center, The University of Tokyo Hospital, 7-3-1 Hongo, Bunkyo-ku, Tokyo 113-8655, Japan; [3]Department of Clinical Neuroscience, The Tokushima University Graduate School of Medicine, 3-18-15 Kuramoto-cho, Tokushima 770-8503, Japan; [4]Department of Neuropathology, Institute for Medical Science of Aging, Aichi Medical University, 21 Karimata, Iwasaku, Nagakute-shi, Aichi 480-1195, Japan; [5]Department of Cell and Developmental Biology, University of Michigan Medical School, 109 Zina Pitcher Place, Ann Arbor, MI 48109-2200, USA; [6]Yoshino Neurology Clinic, 3-3-16 Konodai, Ichikawa, Chiba 272-0827, Japan; [7]Department of Pathology, Graduate School of Medicine, The University of Tokyo, 7-3-1 Hongo, Bunkyo-ku, Tokyo 113-8655, Japan; [8]Department of Neuropathology and the Brain Bank for Aging Research, Tokyo Metropolitan Institute of Gerontology, 35-2 Sakae-cho, Itabashi-ku, Tokyo 173-0015, Japan; [9]Molecular Medicine Laboratory and ANZAC Research Institute, University of Sydney, Sydney NSW 2139, Australia; [10]Department of Neurology, Kyoto University Graduate School of Medicine, 54 Kawahara-cho, Shogoin, Sakyo-ku, Kyoto 606-8507, Japan; [11]Department of Neurology, Nagoya University Graduate School of Medicine, 65 Tsurumai-cho, Showa-ku, Nagoya-shi, Aichi 466-0065, Japan; [12]Department of Neurology and Gerontology, Kyoto Prefectural University Graduate School of Medicine, 465, Kajii-cho, Kamigyo-ku, Kyoto 602-0841, Japan; [13]Division of Applied Genetics, National Institute of Genetics, Yata 1111, Mishima, Shizuoka 11-8540, Japan
*Correspondence: tsuji@m.u-tokyo.ac.jp (S.T.), rkaji@clin.med.tokushima-u.ac.jp (R.K.)
http://dx.doi.org/10.1016/j.ajhg.2012.07.014.

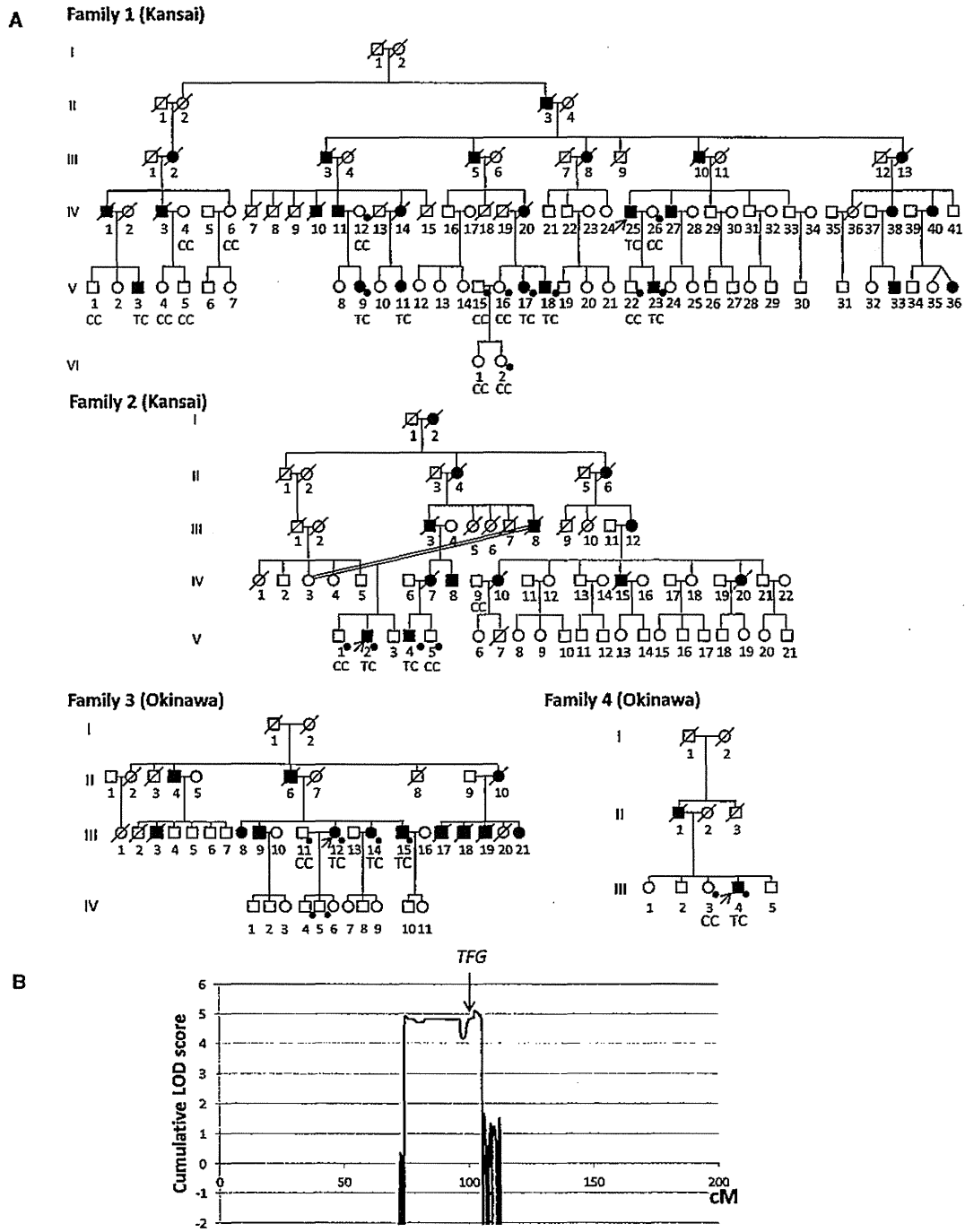

Figure 1. Pedigree Charts and Linkage Analysis

(A) Pedigree charts of families 1 and 2 (Kansai kindreds) and families 3 and 4 (Okinawan kindreds) are shown. Squares and circles indicate males and females, respectively. Affected persons are designated with filled symbols. A diagonal line through a symbol represents a deceased person. A person with an arrow is an index patient. Genotypes of *TFG* c.854 are shown in individuals in whom genomic DNA was analyzed. Individuals genotyped with SNP arrays for linkage analysis and haplotype reconstruction are indicated by dots.
(B) Cumulative parametric multipoint LOD scores on chromosome 3 of all the families are shown.

disease locus to chromosome 3q,[7] overlapping with the previously defined locus, which strongly indicates that these diseases are indeed identical.

In addition to the large Kansai HMSN-P-affected families, we found two new Okinawan HMSN-P-affected families (families 3 and 4 in Figure 1A) in our study. In total, 9 affected and 15 unaffected individuals from the Kansai area and four affected and four unaffected individuals from the Okinawa Islands were enrolled in the study. Written informed consent was obtained from

Table 1. Clinical Characteristics of Patients with HMSN-P from Families 1 and 2 from Kansai and Families 3 and 4 from Okinawa

		Family 3			Family 4
	Families 1 and 2	III-12	III-14	III-15	III-4
Age at examination (years)	40s–50s	54	52	50	54
Age at onset (years)	37.5 ± 8	44	40	early 20s	41
Initial symptoms	shoulder dislocation and difficulty walking	proximal leg weakness	painful cramps	painful cramps and fasciculation	painful cramps and calf atrophy
Motor					
Proximal muscle weakness and atrophy	+	+	mild	+	+
Painful cramps	+	+	+	+	+
Fasciculations	+	+	+	+	+
Motor ability	bedridden after 10–20 years from disease onset	unable to walk; wheelchair	only mild difficulty climbing stairs	walk with effort	unable to walk; wheelchair
Bulbar symptoms	− ~ +	−	−	−	−
Sensory					
Dysesthesia	+	+	mild	+	+
Decreased tactile sensation	+	+	−	mild	+
Decreased vibratory sensation	+	mild	mild	mild	+
Reflexes					
Tendon reflexes	diminished	diminished	diminished	diminished	diminished
Pathological reflexes	−	−	−	−	−
Laboratory Tests and Electrophysiological Findings					
Serum creatine kinase level	270 ± 101 IU/l	761 IU/l	not measured	625 IU/l	399 IU/l
Hyperglycemia	4/13 patients	−	−	−	+
Hyperlipidemia	3/13 patients	+	−	+	+
Nerve conduction study	motor and sensory axonal degeneration	motor and sensory axonal degeneration	not examined	not examined	motor and sensory axonal degeneration
Needle electromyography	neurogenic changes with fibrillation potentials and positive sharp waves	neurogenic changes with fibrillation potentials and positive sharp waves	not examined	not examined	not examined

The clinical characteristics of the patients from families 1 and 2 were summarized in accordance with the previous studies.[5,6]

all participants. This study was approved by the institutional review boards at the University of Tokyo and the Tokushima University Hospital. Genomic DNA was extracted from peripheral-blood leukocytes or an autopsied brain according to standard procedures.

The clinical presentations of the patients from the four families are summarized in Table 1 and Table S1, available online. Characteristic painful cramps and fasciculations were noted at the initial stage of the disease in all the patients from the four families. Whereas some of the patients showed painful cramps in their 20s, the ages of onset of motor weakness (41.6 ± 2.9 years old) were quite uniform. These patients presented slowly progressive, predominantly proximal weakness and atrophy with diminished tendon reflexes in the lower extremities. Sensory impairment was generally mild. Indeed, one patient (III-4 in family 4) has been diagnosed with very slowly progressive ALS. Although frontotemporal dementia (FTD) is an occasionally observed clinical presentation in patients with ALS, dementia was not observed in these patients. Laboratory tests showed mildly elevated serum creatine kinase levels. Electrophysiological studies showed similar results in all the patients investigated and revealed a decreased number of motor units with abundant positive sharp waves, fibrillation, and fasciculation potentials. Sensory-nerve action potentials of the sural nerve were lost in the later stage of the disease. All these clinical findings were similar to those described in previous reports.[1,3,4]

To further narrow the candidate region, we conducted detailed genotyping by employing the Genome-Wide Human SNP array 6.0 (Affymetrix). Multipoint parametric linkage analysis and haplotype reconstruction were performed with the pipeline software SNP-HiTLink[8] and Allegro v.2[9] (Figure 1A). In addition to the SNP genotyping, we also used newly discovered polymorphic dinucleotide repeats for haplotype comparison (microsatellite marker 1 [MS1], chr3: 101,901,207–101,901,249; and MS2, chr3: 102,157,749–102,157,795 in hg18) around *TFG* (see Table S2 for primer sequences). The genome-wide linkage study revealed only one chromosome 3 region showing a cumulative LOD score exceeding 3.0 (Figure 1B), confirming the result of our previous study.[7] An obligate recombination event was observed between rs4894942 and rs1104964, thus further refining the telomeric boundary of the candidate region in Kansai families (Figure 2A). The Okinawan families (families 3 and 4) shared an extended disease haplotype spanning 3.3 Mb, consistent with a founder effect reported in the Okinawan HMSN-P-affected families,[1] thus defining the 3.3 Mb region as the minimum candidate region.

We then performed exon capture (Sequence Capture Human Exome 2.1 M Array [NimbleGen]) of the index patient from family 3 and subsequent passively parallel sequencing by using two lanes of GAIIx (100 bp single end [Illumina]) and a one-fifth slide of SOLiD 4 (50 bp single end [Life Technologies]). GAIIx and SOLiD4 yielded 2.60 and 2.76 Gb of uniquely mapped reads,[10] respectively. The average coverages were 29.0× and 26.8× in GAIIx and SOLiD4, respectively (Table S3 and Figure S1). In summary, 175,236 single nucleotide variants (SNVs) and 25,987 small insertions/deletions were called.[11] The numbers of exonic and splice-site variants were 14,189 and 127, respectively. In the minimum candidate region of 3.3 Mb, only 11 exonic SNVs were found, and only one was novel (i.e., not found in dbSNP) and nonsynonymous. Direct nucleotide-sequence analysis confirmed the presence of heterozygous SNV c.854C>T (p.Pro285Leu) in TRK-fused gene (*TFG* [NM_006070.5]) in all the patients from families 3 and 4 (Figure 3A and Figure S2[12]). Intriguingly, direct nucleotide-sequence analysis of all *TFG* exons (see Table S4 for primer sequences) of one patient from each of families 1 and 2 from the Kansai area revealed an identical c.854C>T (p.Pro285Leu) *TFG* mutation cosegregating with the disease (Figure 1A and Figure 3A). The base substitution was not observed in 482 Japanese controls (964 chromosomes), dbSNP, the 1000 Genomes Project Database, or the Exome Sequencing Project Database. Pro285 is located in the P/Q-rich domain in the C-terminal region of TFG (Figure 3B) and is evolutionally conserved (Figure 3C). PolyPhen predicts it to be "probably damaging." Because some of the exonic sequences were not sufficiently covered by exome sequencing (i.e., their read depths were no more than 10×) (Figure S1), direct nucleotide-sequence analysis was further conducted for these exonic sequences (Table S5). However, it did not reveal any other novel nonsynonymous variants, confirming that c.854C>T (p.Pro285Leu) is the only mutation exclusively present in the candidate region of 3.3 Mb. All together, we concluded that it was the disease-causing mutation.

Because we found an identical mutation in both Kansai (families 1 and 2) and Okinawan (families 3 and 4) families, we then compared the haplotypes with the c.854C>T (p.Pro285Leu) mutation in the Kansai and Okinawan families in detail. To obtain high-resolution haplotypes, we included custom-made markers, including MS1 and MS2, and new SNVs identified by our exome analysis, in addition to the high-density SNPs used in the linkage analysis. The two Kansai families shared as long as 24.0 Mb of haplotype, and the two Okinawan families shared 3.3 Mb, strongly supporting a common ancestry in each region. When the haplotypes of the Kansai and Okinawan families were compared, it turned out that these families do not share the same haplotype because the markers nearest to *TFG* are discordant at markers 48.5 kb centromeric and 677 bp telomeric to the mutation within a haploblock (Figure 2B). Although the possibility of rare recombination events just distal to the mutation cannot be completely excluded, as suggested by the population-based recombination map (Figure 2B), these findings strongly support the interpretation that the mutations have independent origins and provide further evidence that *TFG* contains the causative mutation for this disease.

Mutational analyses of *TFG* were further conducted in patients with other diseases affecting lower motor neurons (including familial ALS [n = 18], axonal HMSN [n = 26], and hereditary motor neuropathy [n = 3]) and revealed no mutations in *TFG*, indicating that c.854C>T (p.Pro285-Leu) in *TFG* is highly specific to HMSN-P.

In this study, we identified in all four families a single variant that appears to have developed on two different haplotypes. The mutation disrupts the PXXP motif, also known as the Src homology 3 (SH3) domain, which might affect protein-protein interactions. In addition, substitution of leucine for proline is expected to markedly alter the protein's secondary structure, which might substantially compromise the physiological functions of TFG.

By employing the primers shown in Table S6, we obtained full-length cDNAs by PCR amplification of the cDNAs prepared from a cDNA library of the human fetal brain (Clontech). During this process, four species of cDNA were identified (Figure S3A). To determine the relative abundance of these cDNA species, we used the primers shown in Table S7 to conduct fragment analysis of the RT-PCR products obtained from RNAs extracted from various tissues; these primers were designed to discriminate four cDNA species on the basis of the size of the PCR products. The analysis revealed that TFG is ubiquitously expressed, including in the spinal cord and dorsal root ganglia, which are the affected sites of HMSN-P (Figure S3B).

Neuropathological studies were performed in a *TFG*-mutation-positive patient (IV-25 in family 1) who died of

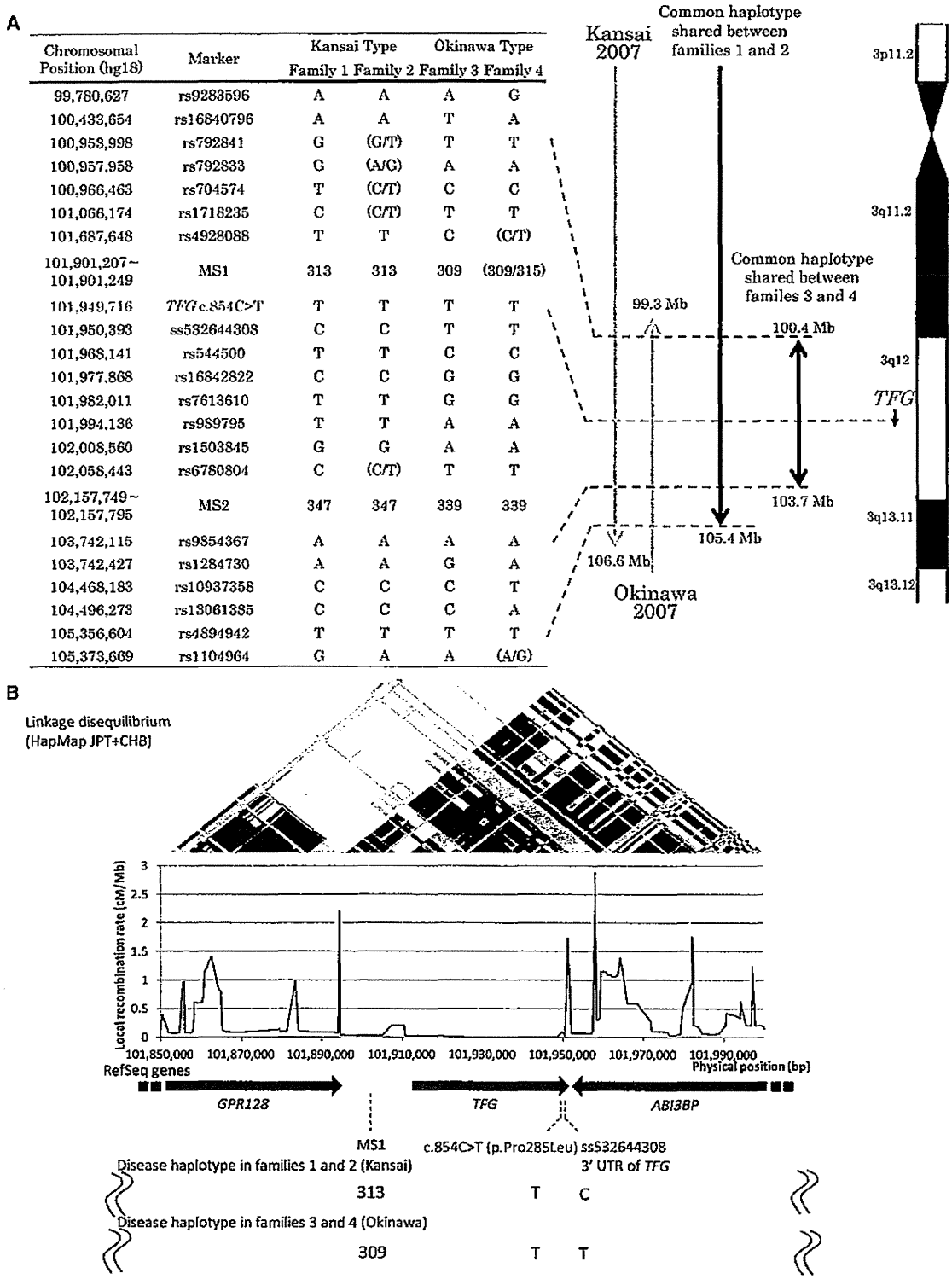

Figure 2. Haplotype Analysis and Minimum Candidate Region of HMSN-P

(A) Haplotypes were reconstructed for all the families with the use of SNP array data and microsatellite markers. Previously reported candidate regions are shown as "Kansai 2007" and "Okinawa 2007."[1,6] Because families 1 and 2 are distantly related, an extended shared common haplotype was observed on chromosome 3, as indicated by a previous study.[6] A reassessment of linkage analysis with high-density SNP markers revealed a recombination between rs4894942 and rs1104964 in family 2, thus refining the telomeric boundary of the candidate region in Kansai families (designated as "Common haplotype shared between families 1 and 2). Furthermore, a shared common haplotype (3.3 Mb with boundaries at rs16840796 and rs1284730) between families 3 and 4 was found, defining the minimum candidate region.

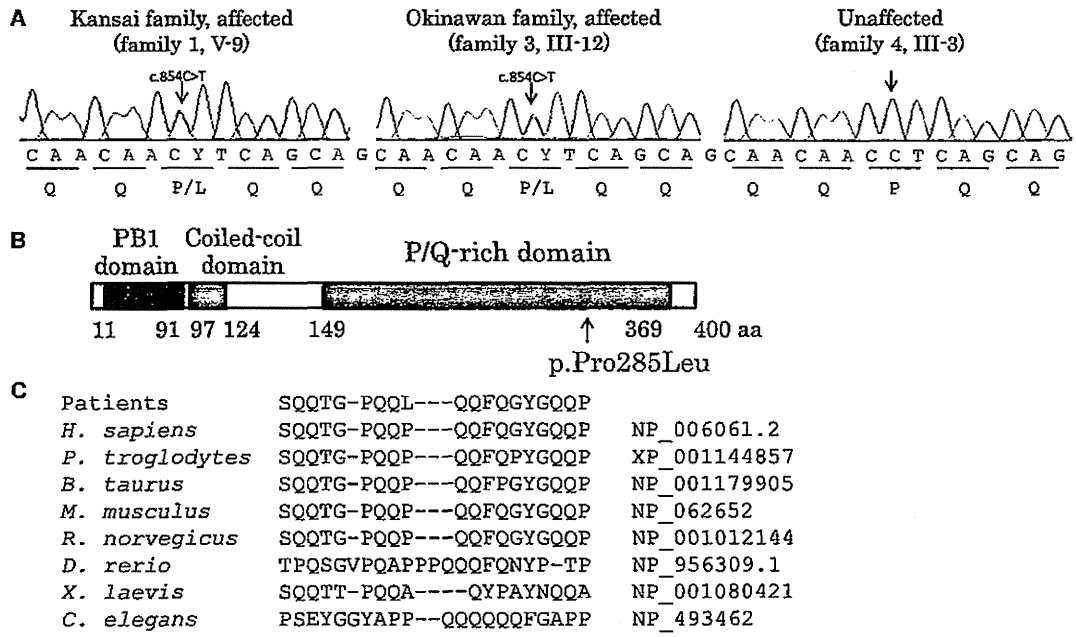

Figure 3. Identification of Causative Mutation
(A) Exome sequencing revealed that only one novel nonsynonymous variant is located within the minimum candidate region. Direct nucleotide-sequence analysis confirmed the mutation, c.854C>T (p.Pro285Leu), in *TFG* in both Kansai and Okinawan families. The mutation cosegregated with the disease (Figure 1A).
(B) Schematic representation of TFG isoform 1. The alteration (p.Pro285Leu) detected in this study is shown below.
(C) Cross-species homology search of the partial TFG amino acid sequence containing the p.Pro285Leu alteration revealed that Pro285 is evolutionally conserved among species.

pneumonia at 67 years of age.[5] Immunohistochemical observations employing a TFG antibody (Table S8) revealed fine granular immunostaining of TFG in the cytoplasm of motor neurons in the spinal cord of neurologically normal controls (n = 3; age at death = 58.7 ± 19.6 years old) (Figure 4A). In the HMSN-P patient, in contrast, TFG-immunopositive inclusion bodies were detected in the motor neurons of the facial, hypoglossal, and abducens nuclei and the spinal cord, as well as in the sensory neurons of the dorsal root ganglia, but were not detected in glial cells (Figures 4B–4D). A small number of cortical neurons in the precentral gyrus also showed TFG-immunopositive inclusion bodies (Figure 4E). Serial sections stained with antibodies against ubiquitin or TFG (Figure 4F) and double immunofluorescence staining (Figure 4G) demonstrated that TFG-immunopositive inclusions colocalized with ubiquitin deposition. Inclusion bodies were immunopositive for optineurin in motor neurons of the brainstem nuclei and the anterior horn of the spinal cord,[5] as well as in sensory neurons of the dorsal root ganglia (data not shown). These data strongly indicate that HMSN-P is a proteinopathy involving TFG.

Because HMSN-P and ALS share some clinical characteristics, we then examined whether neuropathological findings of HMSN-P shared cardinal features with those of sporadic ALS.[13–16] Immunohistochemistry with a TDP-43 antibody revealed skein-like inclusions in the remaining motor neurons of the abducens nucleus and the anterior horn of the lumbar cord (Figures 4H–4I). Phosphorylated TDP-43-positive inclusions were also identified in neurons of the anterior horn of the cervical cord and Clarke's nucleus (Figures 4J–4K). In contrast, TFG immunostaining of spinal-cord specimens from four patients with sporadic ALS (their age at death was 72.3 ± 7.4 years old) revealed no pathological staining in the motor neurons (data not shown). Double immunofluorescence staining revealed that many of the TFG-immunopositive round inclusions in the HSMN-P patient were negative for TDP-43 (Figure 4L), whereas a small number of inclusions were positive for both TFG and TDP-43 (Figure 4M). In addition, to investigate morphological Golgi-apparatus changes, which have recently been found in motor neurons of autopsied tissues of ALS patients,[17] we conducted immunohistochemical analysis by using

(B) Disease haplotypes in the Kansai and Okinawan kindreds are indicated below. Local recombination rates, RefSeq genes, and the linkage disequilibrium map from HapMap JPT (Japanese in Tokyo, Japan) and CHB (Han Chinese in Beijing, China) samples are shown above the disease haplotypes. When disease haplotypes of the Kansai and Okinawan kindreds are compared, the markers nearest to *TFG* are discordant at markers 48.5 kb centromeric and 677 bp telomeric to the mutation within a haploblock, strongly supporting the interpretation that the mutations have independent origins.

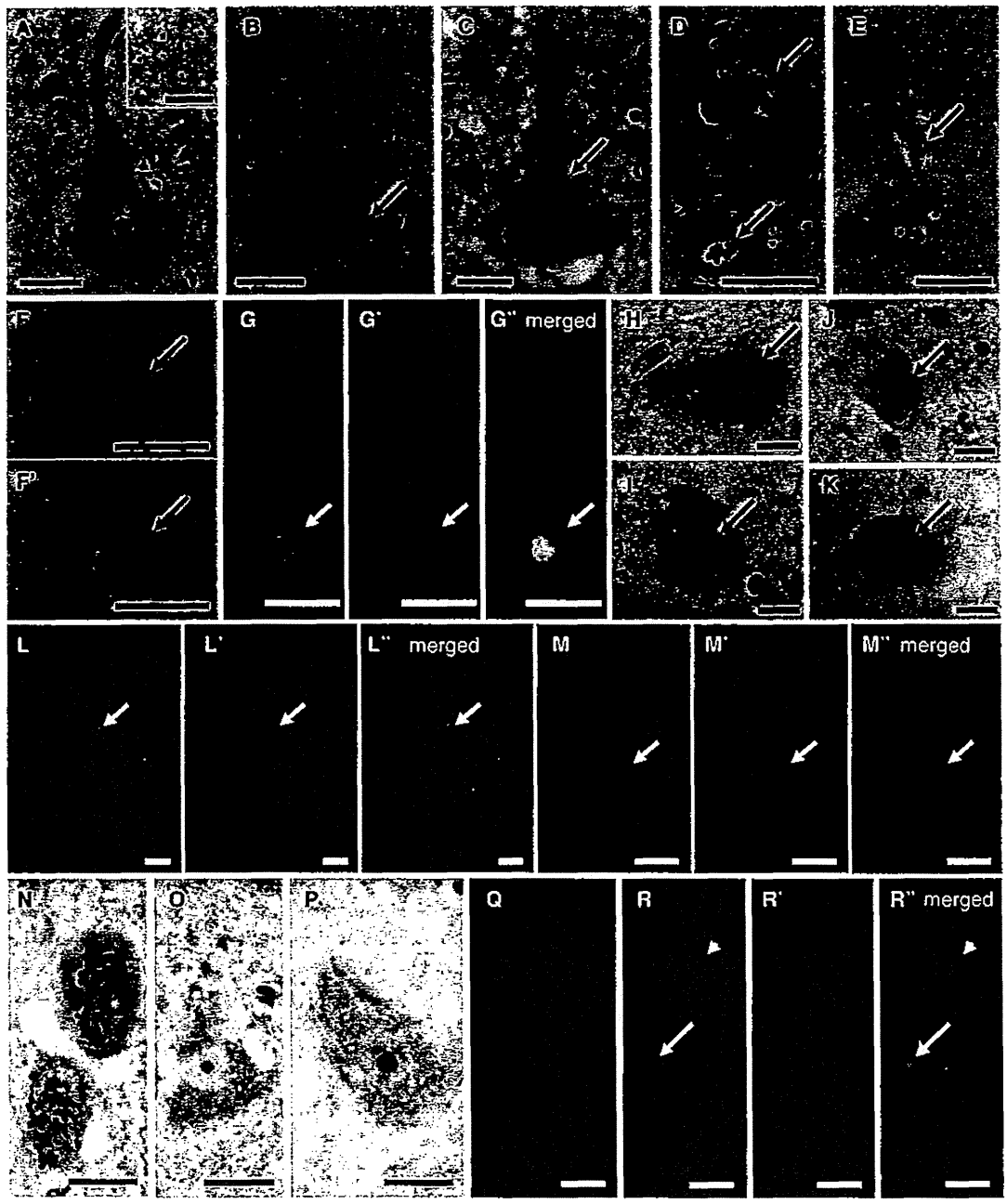

Figure 4. TFG-Related Neuropathological Findings

(A) TFG immunostaining (with hematoxylin counterstaining) of a motor neuron in the spinal cord of a neurologically normal control. A high-power magnified photomicrograph (inset) shows fine granular staining of TFG in the cytoplasm. The scale bars represent 20 μm (main panel) and 10 μm (inset).

(B–E) TFG-immunopositive inclusions of the neurons (with hematoxylin counterstaining) in the hypoglossal nucleus (B), anterior horn of the spinal cord (C), dorsal root ganglion (D, arrows), and motor cortex (E, arrow) of the patient with the *TFG* mutation. The scale bars represent 20 μm (B–D) and 50 μm (E).

(F and F′) Serial section analysis of the facial nucleus motor neuron showing an inclusion body colabeled for TFG (F) and ubiquitin (F′). The scale bars represent 20 μm.

(G–G″) Double immunofluorescence microscopy confirming colocalization of TFG (green) and ubiquitin (red) in an inclusion body of a motor neuron in the hypoglossal nucleus. The scale bars represent 20 μm.

(H and I) TDP-43-positive skein-like inclusions in the motor neurons of the abducens nucleus (H) and anterior horn of the lumbar cord (I). The scale bars represent 20 μm.

(J and K) Phosporylated TDP-43-positive inclusion bodies in the cervical anterior horn (J) and Clarke's nucleus (K). The scale bars represent 20 μm.

(L–L″) Round inclusions (arrows) positive for TFG (green) but negative for TDP-43 (red). The scale bars represent 20 μm.

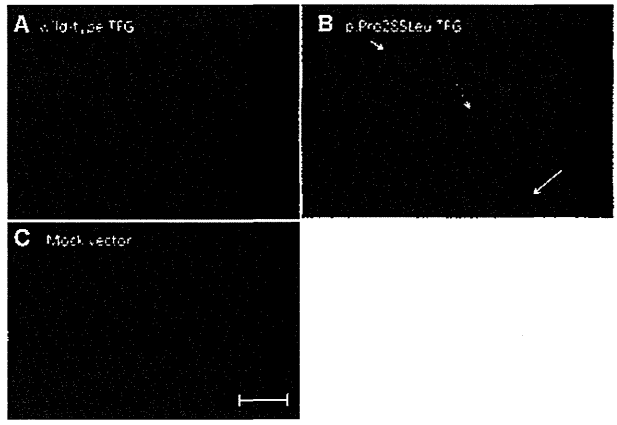

Figure 5. Formation of Cytoplasmic TDP-43 Aggregation Bodies in Cells Stably Expressing Mutant p.Pro285Leu TFG
The coding sequence of *TFG* cDNA was subcloned into pBluescript (Stratagene). After site-directed mutagenesis with a primer pair shown in Table S9, the mutant cDNAs were cloned into the BamHI and XhoI sites of pcDNA3 (Life Technologies). Stable cell lines were established by Lipofectamine (Life Technologies) transfection according to the manufacturer's instructions. Established cell lines were cultured under the ordinary cell-culture conditions (37°C and 5% CO_2) for 5–6 days and were subjected to immunocytochemical analyses. Neuro-2a cells stably expressing wild-type TFG (A), mutant TFG (p.Pro285Leu) (B), and a mock vector (C) are shown. TDP-43-immunopositive cytoplasmic inclusions are absent in the cells stably expressing wild-type TFG or the mock vector (A and C); however, TDP-43-immunopositive cytoplasmic inclusions were exclusively demonstrated in cells stably expressing mutant TFG (p.Pro285Leu), as indicated by arrows (B). Similar results were obtained with HEK 293 cells (not shown). Scale bars represent 10 μm.

a TGN46 antibody. It revealed that the Golgi apparatus was fragmented in approximately 70% of the remaining motor neurons in the lumbar anterior horn. The fragmentation of the Golgi apparatus was prominent near TFG-positive inclusion bodies (Figures 4N–4R). In summary, we found abnormal TDP-43-immunopositive inclusions in the cytoplasm of motor neurons, as well as fragmentation of the Golgi apparatus in HMSN-P, confirming the overlapping neuropathological features between HMSN-P and sporadic ALS.

To further investigate the effect of mutant TFG in cultured cells, stable cell lines expressing wild-type and mutant TFG (p.Pro285Leu) were established from neuro-2a and human embryonic kidney (HEK) 293 cells as previously described.[18] Established cell lines were cultured under the ordinary cell-culture conditions (37°C and 5% CO_2) for 5–6 days and were subjected to immunocytochemical analyses. The neuro-2a cells stably expressing wild-type or mutant TFG demonstrated no distinct difference in the distribution of endogenous TFG, FUS, or OPTN (data not shown). In contrast, cytoplasmic inclusions containing endogenous TDP-43 were exclusively observed in the neuro-2a cells stably expressing untagged mutant TFG, but not in those expressing wild-type TFG (Figure 5). Similar data were obtained from HEK 293 cells (data not shown). Thus, the expression of mutant TFG leads to mislocalization and inclusion-body formation of TDP-43 in cultured cells.

TFG was originally identified as a part of fusion oncoproteins (NTRK1-T3 in papillary thyroid carcinoma,[19] TFG-ALK in anaplastic large cell lymphoma,[20] and TFG/NOR1 in extraskeletal myxoid chondrosarcoma[21]), where the N-terminal portions of TFG are fused to the C terminus of tyrosine kinases or a superfamily of steroid-thyroid hormone-retinoid receptors acting as a transcriptional activator leading to the formation of oncogenic products. Very recently, TFG-1, a homolog of TFG in *Caenorhabditis elegans*, and TFG have been discovered to localize in endoplasmic-reticulum exit sites. TFG-1 acts in a hexameric form that binds the scaffolding protein Sec16 complex assembly and plays an important role in protein secretion with COPII-coated vesicles.[22] It is noteworthy that mutations in genes involved in vesicle trafficking[23,24] (such genes include *VAPB*, *CHMP2B*, *alsin*, *FIG4*, *VPS33B*, *PIP5K1C*, and *ERBB3*) cause motor neuron diseases, emphasizing the role of vesicle trafficking in motor neuron diseases. Thus, altered vesicle trafficking due to the *TFG* mutation might be involved in the motor neuron degeneration in HMSN-P. The presence of TFG-immunopositive inclusions in motor neurons raises the possibility that mutant TFG results in the misfolding and formation of cytoplasmic aggregate bodies, as well as altered vesicle trafficking.

An intriguing neuropathological finding is TDP-43-positive cytoplasmic inclusions in the motor neurons; these inclusions have recently been established as the fundamental neuropathological findings in ALS.[13,14] Of note, expression of mutant, but not wild-type, TFG in cultured cells led to the formation of TDP-43-containing cytoplasmic aggregation. These observations are similar

(M–M″) An inclusion immunopositive for both TFG (green) and TDP-43 (red) is observed in a small number of neurons. The scale bars represent 20 μm.
(N) Normal Golgi apparatus in the neurons of the intact thoracic intermediolateral nucleus. The scale bar represents 20 μm.
(O and P) Fragmentation of the Golgi apparatus with small, round, and disconnected profiles in the affected motor neurons of the lumbar anterior horn. The scale bars represent 20 μm.
(Q–R″) Immunohistochemical observations of the Golgi apparatus and TFG-immunopositive inclusions employing antibodies against TGN46 (red) and TFG (green), respectively. The scale bars represent 10 μm.
(Q) Normal size and distribution (red) in a motor neuron without inclusions.
(R–R″) The Golgi apparatus was fragmented into various sizes and reduced in number in the lumbar anterior horn motor neuron with TFG-positive inclusions (green). The fragmentation predominates near the inclusion (arrow), whereas the Golgi apparatuses distant from the inclusion showed nearly normal patterns (arrow head).

to what has been described for ALS, where TDP-43 is mislocalized from the normally localized nucleus to the cytoplasm with concomitant cytoplasmic inclusions. Cytoplasmic TDP-43 accumulation and inclusion formation have also been observed in motor neurons in familial ALS with mutations in *VAPB* (MIM 608627) or *CHMP2B* (MIM 600795).[25,26] Furthermore, TDP-43 pathology has been demonstrated in transgenic mice expressing mutant VAPB.[27] Although the mechanisms of mislocalization of TDP-43 remain to be elucidated, these observations suggest connections between alteration of vesicle trafficking and mislocalization of TDP-43. Thus, common pathophysiologic mechanisms might underlie motor neuron degenerations involving vesicle trafficking including TFG, as well as VAPB and CHMP2B. Because TDP-43 is an RNA-binding protein, RNA dysregulation has been suggested to play important roles in the TDP43-mediated neurodegeneration.[28] Furthermore, recent discovery of hexanucleotide repeat expansions in *C9ORF72* in familial and sporadic ALS/FTD (MIM 105550)[29,30] emphasizes the RNA-mediated toxicities as the causal mechanisms of neurodegeneration. Observations of TDP-43-positive cytoplasmic inclusions in the motor neurons of the patient with HMSN-P raise the possibility that RNA-mediated mechanisms might also be involved in motor neuron degeneration in HMSN-P.

In summary, we have found that *TFG* mutations cause HMSN-P. The presence of TFG/ubiquitin- and/or TDP-43-immunopositive cytoplasmic inclusions in motor neurons and cytosolic aggregation composed of TDP-43 in cultured cells expressing mutant TFG indicate a novel pathway of motor neuron death.

Supplemental Data

Supplemental Data include three figures and nine tables and can be found with this article online at http://www.cell.com/AJHG/.

Acknowledgments

The authors thank the families for participating in the study. We also thank the doctors who obtained clinical information of the patients. This work was supported in part by Grants-in-Aid for Scientific Research on Innovative Areas (22129002); the Global Centers of Excellence Program; the Integrated Database Project; Scientific Research (A) (B21406026) and Challenging Exploratory Research (23659458) from the Ministry of Education, Culture, Sports, Science, and Technology of Japan; a Grant-in-Aid for Research on Intractable Diseases and Comprehensive Research on Disability Health and Welfare from the Ministry of Health, Labour, and Welfare, Japan; Grants-in-Aid from the Research Committee of CNS Degenerative Diseases; the Ministry of Health, Labour, and Welfare of Japan; the Charcot-Marie-Tooth Association; and the National Medical Research Council of Australia. H.I. was supported by a Research Fellowship from the Japan Society for the Promotion of Science for Young Scientists. We also thank S. Ogawa (Cancer Genomics Project, The University of Tokyo) for his kind help in the analyses employing GAIIx and SOLiD4.

Received: April 16, 2012
Revised: May 27, 2012
Accepted: July 2, 2012
Published online: August 9, 2012

Web Resources

The URLs for data presented herein are as follows.

1000 Genomes Project Database, http://www.1000genomes.org/
dbSNP, http://www.ncbi.nlm.nih.gov/projects/SNP/
HapMap, http://hapmap.ncbi.nlm.nih.gov/
NHLBI GO Exome Sequencing Project, https://esp.gs.washington.edu/drupal/
Online Mendelian Inheritance in Man (OMIM), http://www.omim.org
PolyPhen, http://genetics.bwh.harvard.edu/pph/
RefSeq, http://www.ncbi.nlm.nih.gov/projects/RefSeq/
UCSC Human Genome Browser, http://genome.ucsc.edu/

References

1. Takashima, H., Nakagawa, M., Nakahara, K., Suehara, M., Matsuzaki, T., Higuchi, I., Higa, H., Arimura, K., Iwamasa, T., Izumo, S., and Osame, M. (1997). A new type of hereditary motor and sensory neuropathy linked to chromosome 3. Ann. Neurol. *41*, 771–780.
2. Nakagawa, M. (2009). [Wide spectrum of hereditary motor sensory neuropathy (HMSN)]. Rinsho Shinkeigaku *49*, 950–952.
3. Maeda, K., Sugiura, M., Kato, H., Sanada, M., Kawai, H., and Yasuda, H. (2007). Hereditary motor and sensory neuropathy (proximal dominant form, HMSN-P) among Brazilians of Japanese ancestry. Clin. Neurol. Neurosurg. *109*, 830–832.
4. Patroclo, C.B., Lino, A.M., Marchiori, P.E., Brotto, M.W., and Hirata, M.T. (2009). Autosomal dominant HMSN with proximal involvement: new Brazilian cases. Arq. Neuropsiquiatr. *67* (3B), 892–896.
5. Fujita, K., Yoshida, M., Sako, W., Maeda, K., Hashizume, Y., Goto, S., Sobue, G., Izumi, Y., and Kaji, R. (2011). Brainstem and spinal cord motor neuron involvement with optineurin inclusions in proximal-dominant hereditary motor and sensory neuropathy. J. Neurol. Neurosurg. Psychiatry *82*, 1402–1403.
6. Takahashi, H., Makifuchi, T., Nakano, R., Sato, S., Inuzuka, T., Sakimura, K., Mishina, M., Honma, Y., Tsuji, S., and Ikuta, F. (1994). Familial amyotrophic lateral sclerosis with a mutation in the Cu/Zn superoxide dismutase gene. Acta Neuropathol. *88*, 185–188.
7. Maeda, K., Kaji, R., Yasuno, K., Jambaldorj, J., Nodera, H., Takashima, H., Nakagawa, M., Makino, S., and Tamiya, G. (2007). Refinement of a locus for autosomal dominant hereditary motor and sensory neuropathy with proximal dominancy (HMSN-P) and genetic heterogeneity. J. Hum. Genet. *52*, 907–914.
8. Fukuda, Y., Nakahara, Y., Date, H., Takahashi, Y., Goto, J., Miyashita, A., Kuwano, R., Adachi, H., Nakamura, E., and Tsuji, S. (2009). SNP HiTLink: A high-throughput linkage analysis system employing dense SNP data. BMC Bioinformatics *10*, 121.
9. Gudbjartsson, D.F., Thorvaldsson, T., Kong, A., Gunnarsson, G., and Ingolfsdottir, A. (2005). Allegro version 2. Nat. Genet. *37*, 1015–1016.

10. Li, H., and Durbin, R. (2009). Fast and accurate short read alignment with Burrows-Wheeler transform. Bioinformatics *25*, 1754–1760.
11. Li, H., Handsaker, B., Wysoker, A., Fennell, T., Ruan, J., Homer, N., Marth, G., Abecasis, G., and Durbin, R.; 1000 Genome Project Data Processing Subgroup. (2009). The Sequence Alignment/Map format and SAMtools. Bioinformatics *25*, 2078–2079.
12. Robinson, J.T., Thorvaldsdóttir, H., Winckler, W., Guttman, M., Lander, E.S., Getz, G., and Mesirov, J.P. (2011). Integrative genomics viewer. Nat. Biotechnol. *29*, 24–26.
13. Neumann, M., Sampathu, D.M., Kwong, L.K., Truax, A.C., Micsenyi, M.C., Chou, T.T., Bruce, J., Schuck, T., Grossman, M., Clark, C.M., et al. (2006). Ubiquitinated TDP-43 in frontotemporal lobar degeneration and amyotrophic lateral sclerosis. Science *314*, 130–133.
14. Arai, T., Hasegawa, M., Akiyama, H., Ikeda, K., Nonaka, T., Mori, H., Mann, D., Tsuchiya, K., Yoshida, M., Hashizume, Y., and Oda, T. (2006). TDP-43 is a component of ubiquitin-positive tau-negative inclusions in frontotemporal lobar degeneration and amyotrophic lateral sclerosis. Biochem. Biophys. Res. Commun. *351*, 602–611.
15. Hasegawa, M., Arai, T., Nonaka, T., Kametani, F., Yoshida, M., Hashizume, Y., Beach, T.G., Buratti, E., Baralle, F., Morita, M., et al. (2008). Phosphorylated TDP-43 in frontotemporal lobar degeneration and amyotrophic lateral sclerosis. Ann. Neurol. *64*, 60–70.
16. Inukai, Y., Nonaka, T., Arai, T., Yoshida, M., Hashizume, Y., Beach, T.G., Buratti, E., Baralle, F.E., Akiyama, H., Hisanaga, S., and Hasegawa, M. (2008). Abnormal phosphorylation of Ser409/410 of TDP-43 in FTLD-U and ALS. FEBS Lett. *582*, 2899–2904.
17. Stieber, A., Chen, Y., Wei, S., Mourelatos, Z., Gonatas, J., Okamoto, K., and Gonatas, N.K. (1998). The fragmented neuronal Golgi apparatus in amyotrophic lateral sclerosis includes the trans-Golgi-network: Functional implications. Acta Neuropathol. *95*, 245–253.
18. Kuroda, Y., Sako, W., Goto, S., Sawada, T., Uchida, D., Izumi, Y., Takahashi, T., Kagawa, N., Matsumoto, M., Matsumoto, M., et al. (2012). Parkin interacts with Klokin1 for mitochondrial import and maintenance of membrane potential. Hum. Mol. Genet. *21*, 991–1003.
19. Greco, A., Mariani, C., Miranda, C., Lupas, A., Pagliardini, S., Pomati, M., and Pierotti, M.A. (1995). The DNA rearrangement that generates the TRK-T3 oncogene involves a novel gene on chromosome 3 whose product has a potential coiled-coil domain. Mol. Cell. Biol. *15*, 6118–6127.
20. Hernández, L., Pinyol, M., Hernández, S., Beà, S., Pulford, K., Rosenwald, A., Lamant, L., Falini, B., Ott, G., Mason, D.Y., et al. (1999). TRK-fused gene (TFG) is a new partner of ALK in anaplastic large cell lymphoma producing two structurally different TFG-ALK translocations. Blood *94*, 3265–3268.
21. Hisaoka, M., Ishida, T., Imamura, T., and Hashimoto, H. (2004). TFG is a novel fusion partner of NOR1 in extraskeletal myxoid chondrosarcoma. Genes Chromosomes Cancer *40*, 325–328.
22. Witte, K., Schuh, A.L., Hegermann, J., Sarkeshik, A., Mayers, J.R., Schwarze, K., Yates, J.R., 3rd, Eimer, S., and Audhya, A. (2011). TFG-1 function in protein secretion and oncogenesis. Nat. Cell Biol. *13*, 550–558.
23. Dion, P.A., Daoud, H., and Rouleau, G.A. (2009). Genetics of motor neuron disorders: New insights into pathogenic mechanisms. Nat. Rev. Genet. *10*, 769–782.
24. Andersen, P.M., and Al-Chalabi, A. (2011). Clinical genetics of amyotrophic lateral sclerosis: What do we really know? Nat Rev Neurol *7*, 603–615.
25. Ince, P.G., Highley, J.R., Kirby, J., Wharton, S.B., Takahashi, H., Strong, M.J., and Shaw, P.J. (2011). Molecular pathology and genetic advances in amyotrophic lateral sclerosis: an emerging molecular pathway and the significance of glial pathology. Acta Neuropathol. *122*, 657–671.
26. Cox, L.E., Ferraiuolo, L., Goodall, E.F., Heath, P.R., Higginbottom, A., Mortiboys, H., Hollinger, H.C., Hartley, J.A., Brockington, A., Burness, C.E., et al. (2010). Mutations in CHMP2B in lower motor neuron predominant amyotrophic lateral sclerosis (ALS). PLoS ONE *5*, e9872.
27. Tudor, E.L., Galtrey, C.M., Perkinton, M.S., Lau, K.-F., De Vos, K.J., Mitchell, J.C., Ackerley, S., Hortobágyi, T., Vámos, E., Leigh, P.N., et al. (2010). Amyotrophic lateral sclerosis mutant vesicle-associated membrane protein-associated protein-B transgenic mice develop TAR-DNA-binding protein-43 pathology. Neuroscience *167*, 774–785.
28. Lee, E.B., Lee, V.M., and Trojanowski, J.Q. (2012). Gains or losses: Molecular mechanisms of TDP43-mediated neurodegeneration. Nat. Rev. Neurosci. *13*, 38–50.
29. DeJesus-Hernandez, M., Mackenzie, I.R., Boeve, B.F., Boxer, A.L., Baker, M., Rutherford, N.J., Nicholson, A.M., Finch, N.A., Flynn, H., Adamson, J., et al. (2011). Expanded GGGGCC hexanucleotide repeat in noncoding region of C9ORF72 causes chromosome 9p-linked FTD and ALS. Neuron *72*, 245–256.
30. Renton, A.E., Majounie, E., Waite, A., Simón-Sánchez, J., Rollinson, S., Gibbs, J.R., Schymick, J.C., Laaksovirta, H., van Swieten, J.C., Myllykangas, L., et al; ITALSGEN Consortium. (2011). A hexanucleotide repeat expansion in C9ORF72 is the cause of chromosome 9p21-linked ALS-FTD. Neuron *72*, 257–268.

Journal of the Peripheral Nervous System 17:206–209 (2012)

CASE REPORT

A novel *EGR2* mutation within a family with a mild demyelinating form of Charcot-Marie-Tooth disease

Kensuke Shiga[1], Yuichi Noto[1], Ikuko Mizuta[1], Akihiro Hashiguchi[2], Hiroshi Takashima[2], and Masanori Nakagawa[1]

[1] *Department of Neurology, Kyoto Prefectural University of Medicine, Graduate School of Medicine, Kyoto and* [2] *Department of Neurology and Geriatrics, Kagoshima University, Graduate School of Medical and Dental Sciences, Kagoshima, Japan*

Abstract Mutations of the early growth response 2 (*EGR2*) gene have been reported in a variety of severe demyelinating neuropathies such as autosomal recessive congenital hypomyelinating neuropathy, autosomal dominant child-onset Dejerine-Sottas neuropathy, and autosomal dominant adult-onset Charcot-Marie-Tooth disease (CMT). Here, we report on a heterozygous mutation in *EGR2* (c.1160C>A), which results in threonine at position 387 being changed to asparagine, in a family with a mild demyelinating form of adult-onset CMT. Of note, both the proband and her asymptomatic son exhibited neither pes cavus nor champagne-bottle leg atrophy, suggesting that the heterozygous T387N mutation may result in a relatively mild phenotype of demyelinating CMT.

Key words: Charcot-Marie-Tooth disease, demyelinating neuropathy, *EGR2* mutation, heterozygous mutation, mild phenotype

Introduction

Subtype of CMT and associated gene mutation

This case report chronicles a family with autosomal dominant demyelinating Charcot-Marie-Tooth disease (CMT) and mutations in the early response 2 gene (*EGR2*) (CMT1D, OMIM 607678).

Description of the case

The proband was a 46-year-old woman who had been healthy until 2 years ago, when she noticed a subtle tingling sensation on the dorsal aspect of her left hand. One year later, she started to have difficulty screwing off bottle caps and visited our facility. The proband was the only daughter of a father who died due to gastric cancer at 59 years of age and a mother who died due to diabetes at 63 years of age; neither parent had neuromuscular disease, but the mother was known to be a slow runner. The patient had three sons: the eldest was a 24-year-old part-time worker, the second was a 19-year-old office worker, and the youngest was a 16-year-old high school student. All of them were able to run, but the second son was a slow runner when he was a student.

Neurological examination of the proband revealed that the cranial nerves were normal. The left thenar prominence showed mild atrophy; however, neither hammer toes nor pes cavus were noticed. The Medical Research Council (MRC) scores were 4 in the abductor pollicis brevis, tibialis anterior, and extensor hallucis longus muscles, and 5 in the other muscles. Sensations were preserved except for subtle paresthesias on the dorsal aspect of her left hand. Both patellar tendon reflexes and Achilles tendon reflexes were absent, whereas reflexes were preserved in the upper extremities.

The results of nerve conduction studies (NCS) of the proband are shown in Table 1. Distal motor

Address correspondence to: Kensuke Shiga, MD, Department of Neurology, Kyoto Prefectural University of Medicine, Graduate School of Medicine, Kajiicho 465, Kamigyo-ku, Kyoto 602-8566, Japan. Tel: +81-75-251-5793; Fax: +81-75-211-8645; E-mail: kenshiga@koto.kpu-m.ac.jp

Table 1. Results of the motor nerve conduction and sensory nerve conduction studies in the proband.

	Median nerve, right	Ulnar nerve, right	Tibial nerve, right
Motor nerve conduction study			
Distal latency (ms)	5.96	4.12	6.72
CMAP (mV)	7.33	10.18	7.28
Duration (ms)	6.16	6.14	7.36
MCV (m/s), distal segments	24.0	28.9	23.2
MCV (m/s), proximal segments	26.1	25.9	—
Sensory nerve conduction study			
SNAP (μV)	1.3	0.9	Not evoked
SCV (m/s)	29.6	32.9	—

The distal median nerve MCV was measured between the wrist and elbow, whereas the proximal median nerve MCV was measured between the elbow and axilla. The distal ulnar nerve MCV was measured between the wrist and below the elbow and the proximal ulnar nerve MCV was measured below and above the elbow. The tibial nerve MCV was measured between the ankle and popliteal fossa. SCVs were measured between the wrist and the index and between the wrist and little fingers in the median and ulnar nerves, respectively, and between the LM and the distal shin 14 cm proximal to the LM.
CMAP, compound muscle action potential; LM, lateral malleolus; MCV, motor conduction velocity; SCV, sensory conduction velocity; SNAP, sensory nerve action potential.

latencies were prolonged in the median, ulnar, and tibial nerves. The motor nerve conduction velocities (MCVs) of these nerves were decreased equally in both the distal and proximal segments and the electric thresholds were markedly increased elsewhere. On the other hand, the compound muscle action potentials were relatively preserved. In the sensory NCS, sensory nerve action potentials (SNAPs) were markedly reduced or were not elicitable. The symmetric and uniform slowing of MCVs in a length-dependent manner suggested dysmyelination, the developmental defect in myelination, favoring a diagnosis of CMT1 (demyelinating form).

After obtaining a written informed consent from the patient, DNA was extracted from the proband's lymphocytes and was subjected to fluorescence *in situ* hybridization analysis for peripheral myelin protein (*PMP22*) duplication. Results showed the presence of the normal two copies of the gene. DNA was then analyzed further using a custom-built GeneChip® CustomSeq® Resequencing Array (Affimetrix, Santa Clara, CA, USA). This array was designed to screen for the following 28 CMT-related genes: *PMP22, myelin protein zero* (*MPZ*), *gap junction protein beta 1* (*GJB1*), *EGR2, periaxin* (*PRX*), *lipopolysaccharide-induced TNF factor* (*LITAF*), *neurofilament light chain* (*NEFL*), *ganglioside-induced differentiation association protein 1* (*GDAP1*), *myotubularin-related protein 2* (*MTMR2*), *SH3 domain and tetratricopeptide repeats 2* (*SH3TC2*), *SET-binding factor 2* (*SBF2*), *N-myc downstream regulated 1* (*NDRG1*), *mitofusin 2* (*MFN2*), *rab-protein 7* (*RAB7*), *glycyl-tRNA synthetase* (*GARS*), *heat shock 27 kDa protein 1* (*HSPB1*), *heat shock 22 kDa protein 8* (*HSPB8*), *lamin A/C* (*LMNA*), *dynamin 2* (*DNM2*), *tyrosyl-tRNA synthetase* (*YARS*), *alanyl-tRNA synthetase* (*AARS*), *lysyl-tRNA synthetase* (*KARS*), *aprataxin* (*APTX*), *senataxin* (*SETX*), *tyrosyl-DNA phosphodiesterase 1* (*TDP1*), *desert hedgehog* (*DHH*), *gigaxonin 1* (*GAN1*), and *K-Cl cotransporter family 2* (*KCC3*). The technical details of the array have been described in another publication *(Nakamura et al., 2012)*. The authors had obtained the approval of the genetic analysis using GeneChip from the institutional review boards of both institutions (Kyoto Prefectural University of Medicine and University of Kagoshima). The results showed a novel heterozygous mutation in *EGR2* (c.1160C>A) resulting in change of threonine at position 387 to asparagine (Fig. 1). To elucidate the pathogenicity of this mutation, we performed familial segregation analysis. The proband and all her sons agreed to participate in the study on written informed consent. Neurological examination of the second son unexpectedly revealed mild weakness of the extensor hallucis longus and tibialis anterior muscles, with an MRC score of 4. In addition, he had diminished patellar and Achilles tendon reflexes. In contrast, the eldest and youngest sons had normal neurological examination findings. The results of NCS for the right median nerve of the proband and her three sons are shown in Table 2. The median MCVs were decreased to 21.5 and 19.5 m/s in the proband and her second son, respectively, whereas those of the eldest and youngest sons were within the normal range. In addition, median SNAPs and sensory conduction velocities were also decreased in the proband and her second son, but remained normal in the other sons. The direct sequencing of *EGR2* revealed a heterozygous c.1160C>A mutation in the second son and a homozygous wild-type sequence in the other sons (Fig. 1). In summary, the heterozygous mutation of *EGR2* (c.1160C>A) was associated with a mild demyelinating neuropathy phenotype in this family.

Discussion

EGR2 is a "master" transcription factor that regulates myelination of the peripheral nervous system and plays a role in the maintenance of myelin *(Topilko et al., 1994; Warner et al., 1998)*. Genetic alteration of *EGR2* results in a variety of relatively severe demyelinating neuropathies such as congenital hypomyelinating neuropathy *(Warner et al., 1998)*, childhood-onset Dejerine-Sottas neuropathy (DSN)

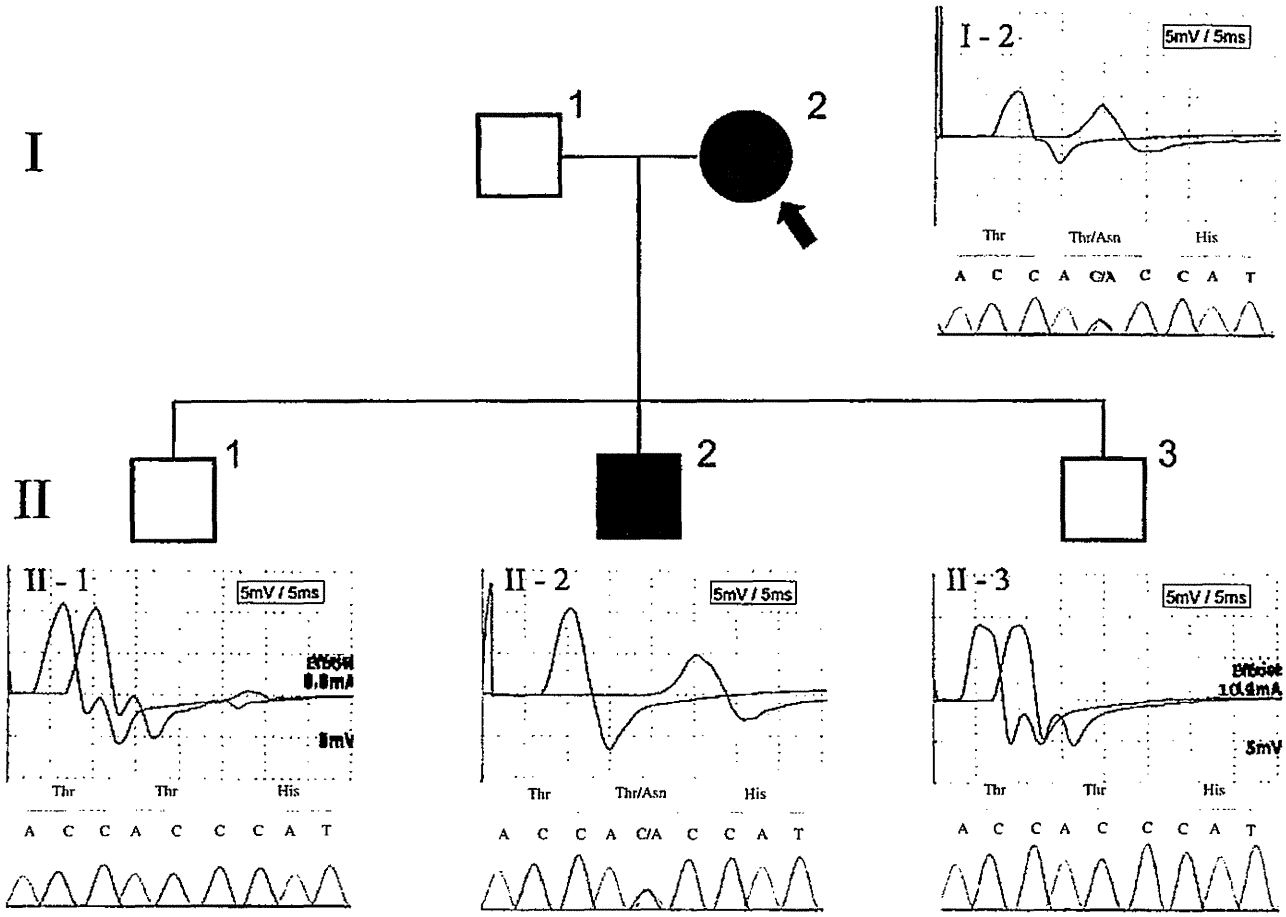

Figure 1. Family segregation study. I-2 (closed arrow): the proband, II-1: eldest son, II-2: second son, III-3: youngest son. Compound muscle action potentials (CMAPs) elicited by supramaximal stimulation of the right median nerve at the wrist and elbow were obtained for each family member, and these CMAPs were superimposed on each other. The onset of CMAPs was delayed in both I-2 and II-2. The chromatograms of the direct sequencing of exon 2 of early response 2 gene (*EGR2*) are shown below. A heterozygous c.1160C>A mutation was noted in both I-2 and II-2.

Table 2. Motor nerve and sensory nerve conductions in the median nerve of the proband and her sons.

Family member	I-2	II-1	II-2	II-3
Motor nerve conduction				
Distal latency (ms) (<4.2)	6.6	2.8	6.7	3.0
CMAP (mV) (>3.5)	5.4	10.7	10.4	8.9
MCV* (m/s) (>48)	21.5	56.1	19.0	57.6
Sensory nerve conduction				
SNAP (μV) (>19)	1.1	43.3	1.8	30.8
SCV† (m/s) (>47)	25.2	62.0	25.4	55.6

CMAP, compound muscle action potential; I-2 (closed arrow in Fig. 1), the proband; II-1, eldest son; II-2, second son; III-3, youngest son; MCV, motor conduction velocity; SCV, sensory conduction velocity; SNAP, sensory nerve action potential.
*MCVs were measured between the wrist and elbow.
†SCVs were measured between the wrist and index finger in the median nerves.

(Boekoel et al., 2001; Numakura et al., 2003; Szigeti et al., 2007), and adult-onset CMT type 1 *(Warner et al., 1998; Bellone et al., 1999; Yoshihara et al., 2001; Vandenberghe et al., 2002; Mikesová et al., 2005)*. In contrast, the proband in this report exhibited a rather milder phenotype, without typical features of CMT, such as champagne-bottle leg atrophy or pes cavus.

We consider c.1160C>A (p. Thr387Asn) in *EGR2* in the proband to be pathogenic for the following reasons. First, the amino acid alteration was clearly segregated in this family both with the reduced MCVs and with the mild neuropathic phenotype. Second, the nucleotide variation (c.1160C>A) has not been reported either in the dbSNP database or in the 1,000 genome catalog (as of January 2012). Third, the 387th amino acid threonine, located in the second zinc-finger domain of the EGR2 protein, is well conserved among different species ranging from humans to zebra fish. We thus assume that this amino acid alteration can affect the DNA-binding capacity of the protein transcription factor, possibly leading to